Title	Downregulation of the Wnt antagonist Dkk2 links the loss of Sept4 and myofibroblastic transformation of hepatic stellate cells.
Author(s)	Yanagida, Atsuko; Iwaisako, Keiko; Hatano, Etsuro; Taura, Kojiro; Sato, Fumiaki; Narita, Masato; Nagata, Hiromitsu; Asechi, Hiroyuki; Uemoto, Shinji; Kinoshita, Makoto
Citation	Biochimica et biophysica acta (2011), 1812(11): 1403-1411
Issue Date	2011-11
URL	http://hdl.handle.net/2433/149268
Right	© 2011 Elsevier B.V.
Type	Journal Article
Textversion	author

Downregulation of the Wnt antagonist Dkk2 links the loss of Sept4 and myofibroblastic

transformation of hepatic stellate cells

Atsuko Yanagida[a,b,f], Keiko Iwaisako[a,b,c,f], Etsuro Hatano[a], Kojiro Taura[a,c], Fumiaki

Sato[d], Masato Narita[a], Hiromitsu Nagata[a], Hiroyuki Asechi[a], Shinji Uemoto[a], Makoto

Kinoshita[b,e]

[a]Department of Surgery, Graduate School of Medicine, Kyoto University, 54

Kawahara-cho, Shogoin, Sakyo-ku, Kyoto 606 8507, Japan

[b]Biochemistry and Cell Biology Unit, Graduate School of Medicine, Kyoto University,

Yoshida-Konoe, Sakyo-ku, Kyoto 606 8501, Japan

[c]Department of Medicine, University of California, San Diego, 9500 Gilman DR #0702,

La Jolla, CA 92093, USA

[d]Department of Nanobio Drug Discovery, Graduate School of Pharmacology, Kyoto

University, 46-29 Shimoadachi-cho, Yoshida, Sakyo-ku, Kyoto 606 8501, Japan

[e]Division of Biological Science, Graduate School of Science, Nagoya University,

Furo-cho, Chikusa-ku, Nagoya 464 8602, Japan

[f]These authors contributed equally to this paper.

E-mail addresses

Atsuko Yanagida: atsukoya@kuhp.kyoto-u.ac.jp

Keiko Iwaisako: iwaisako@kuhp.kyoto-u.ac.jp

Etsuro Hatano: etsu@kuhp.kyoto-u.ac.jp

Kojiro Taura: ktaura@kuhp.kyoto-u.ac.jp

Fumiaki Sato: fsato@pharm.kyoto-u.ac.jp

Masato Narita: narinari@kuhp.kyoto-u.ac.jp

Hiromitsu Nagata: hiromitu@kuhp.kyoto-u.ac.jp

Hiroyuki Asechi: asechi@kuhp.kyoto-u.ac.jp

Shinji Uemoto: uemoto@kuhp.kyoto-u.ac.jp

Makoto Kinoshita: kinoshita.makoto@c.mbox.nagoya-u.ac.jp

Corresponding author: Dr. Etsuro Hatano

Department of Surgery, Graduate School of Medicine, Kyoto University, 54

Kawahara-cho, Shogoin, Sakyo-ku, Kyoto 606 8507, Japan

Telephone: +81-75-751-4323

Fax: +81-75-751-4348

E-mail: etsu@kuhp.kyoto-u.ac.jp

ABSTRACT

Background/Aims: Sept4, a subunit of the septin cytoskeleton specifically expressed in quiescent hepatic stellate cells (HSCs), is downregulated through transdifferentiation to fibrogenic and contractile myofibroblastic cells. Since $Sept4^{-/-}$ mice are prone to liver fibrosis, we aimed to identify the unknown molecular network underlying liver fibrosis by probing the association between loss of *Sept4* and accelerated transdifferentiation of HSCs. *Methods*: We compared the transcriptomes of $Sept4^{+/+}$ and $Sept4^{-/-}$ HSCs undergoing transdifferentiation by DNA microarray and quantitative reverse transcription polymerase chain reaction (RT-PCR) analysis. Because *Dickkopf2* (*Dkk2*) gene expression is reduced in $Sept4^{-/-}$ HSCs, we tested whether supplementing Dkk2 could suppress myofibroblastic transformation of $Sept4^{-/-}$ HSCs. We tested the involvement of the canonical Wnt pathway in this process by using a lymphoid enhancer-binding factor/transcription factor-luciferase reporter assay. *Results*: We observed consistent upregulation of *Dkk2* in primary cultured HSCs and in a carbon tetrachloride liver fibrosis in mice, which was decreased in the absence of *Sept4*. Supplementation with Dkk2 suppressed the induction of pro-fibrotic genes (*α-smooth muscle actin* and 2 collagen genes) and induced an anti-fibrotic gene (*Smad7*) in $Sept4^{-/-}$ HSCs. In human liver specimens with inflammation and fibrosis, Dkk2

immunoreactivity appeared to be positively correlated with the degree of fibrotic changes. ***Conclusions***: Pro-fibrotic transformation of HSCs through the loss of *Sept4* is, in part, due to reduced expression of *Dkk2* and its homologues, and the resulting disinhibition of the canonical Wnt pathway.

Keywords: septin, hepatic stellate cell, canonical Wnt pathway, Dkk (Dickkopf), myofibroblastic transformation, liver fibrosis

Abbreviations: HSCs (hepatic stellate cells), RT-PCR (reverse transcription polymerase chain reaction), α-Sma (α-smooth muscle actin), Dkk (Dickkopf), Fzd (Frizzled), LRP (low density lipoprotein receptor-related protein), Lef/Tcf (lymphoid enhancer-binding factor/transcription factor), DMEM (Dulbecco's Modified Eagle's Medium), FBS (fetal bovine serum), CCl_4 (carbon tetrachloride), DIV (day in vitro), sFRPs (secreted frizzled-related proteins), TGF-β (transforming growth factor β), SOCS7 (suppressor of cytokine signaling 7), NCK (non-catalytic region of tyrosine kinase adaptor protein)

1. Introduction

Chronic liver inflammation caused by viral infections, alcohol and other toxic chemicals, and metabolic disorders is accompanied by tissue remodeling and fibrosis. These interrelated pathological processes are major issues in hepatology because they are implicated in major clinical disorders, namely liver cirrhosis and carcinoma. Previous studies have highlighted hepatic stellate cells (HSCs) as pivotal players contributing to liver fibrosis [1, 2]. Upon liver damage, HSCs transdifferentiate into myofibroblastic cells by inflammatory cytokines released mainly from Kupffer cells (KCs). Transformed HSCs are distinct from quiescent HSCs in terms of their proliferative activity, contractility facilitated by *α-smooth muscle actin (α-SMA)* expression, and production of collagens and other extracellular matrices. Since these properties contribute to the pathogenesis of liver fibrosis and cirrhosis, the molecular mechanism underlying myofibroblastic transformation of HSCs has been a research focus in this field.

Septins are a family of cytoskeletal/scaffold proteins ubiquitously expressed in eukaryotic cells. Among the 13 septin genes shared by mice and humans, *Sept4* is unique in that it is expressed in specific cells such as Bergmann glial cells in the

cerebellum, dopamine neurons in the midbrain, and spermatozoa. Loss of *Sept4* causes disparate phenotypes in these systems [3, 4].

We previously reported that *Sept4* is expressed exclusively in quiescent HSCs in the liver, it is strongly downregulated through transdifferentiation of HSCs in vitro*,* and Sept4 protein is undetectable in HSCs in human specimens with liver fibrosis. Since *Sept4*$^{-/-}$ mice are prone to liver fibrosis, the presence of Sept4 contributes to the suppression of myofibroblastic transformation of HSCs by unknown mechanisms [5]. In this study, we examined the accelerated transdifferentiation of HSCs in *Sept4*$^{-/-}$ mice attempting to identify the unknown molecular network underlying liver fibrosis and the physiological role of Sept4 in HSCs.

By comparing the transcriptomes of HSCs collected from *Sept4*$^{+/+}$ and *Sept4*$^{-/-}$ mice, we found reproducible differences. Here, we focus on *Dickkopf2* (*Dkk2*) and its homologues. We found that *Dkk2* is expressed specifically in HSCs, that it is upregulated through myofibroblastic transformation in vivo and in vitro, and that the *Dkk* upregulation is diminished in *Sept4*$^{-/-}$ HSCs. Previous studies from other groups have shown that the canonical Wnt pathway promotes fibrosis of the liver, kidney, lung, and other tissues [6-9], which is countered by Dkks that interfere with the interaction between Wnt proteins, the cognate membrane-bound receptor Frizzled (Fzd), and

LRP5/6 (low-density lipoprotein receptor-related protein 5/6) [10-12]. On the basis of

the above information and our own data, we conclude that pro-fibrotic transformation of

HSCs in the absence of Sept4 is, at least in part, due to the reduced upregulation of *Dkk*

genes and the resulting disinhibition of the canonical Wnt pathway.

2. Materials and Methods

2.1. Animals

Characterization of $Sept4^{-/-}$ mice with a C57BL/6J background has been reported

previously [3-5]. The protocol for animal handling was reviewed and approved by the

Animal Care and Use Committee of Kyoto University.

2.2. Liver cell fractionation and cell culture

We fractionated HSCs from $Sept4^{+/+}$ or $Sept4^{-/-}$ male mice using a standard

method with some modifications [5, 13]. In brief, we dispersed liver cells by infusing

0.025% Pronase E (Kaken Pharmaceutical, Tokyo, Japan) and 0.025% collagenase

(Wako, Osaka, Japan) in SC-2 solution (137 mM NaCl, 5.4 mM KCl, 0.57 mM

NaH_2PO_4, 0.85 mM Na_2HPO_4, 10 mM HEPES, 4.2 mM $NaHCO_3$, and 3.8 mM $CaCl_2$

[pH 7.25]). The collected liver cells were centrifuged on an 8.0% Nycodenz (Nycomed

Pharma, Oslo, Norway) cushion. The density-separated HSCs were grown on uncoated

dishes in Dulbecco's Modified Eagle's Medium (DMEM) supplemented with 10% fetal

bovine serum (FBS) and antibiotics in 5% CO_2 at 37ºC. The purity of HSCs was

consistently more than 98%, as assessed by the presence of lipid droplets and

autofluorescence of vitamin A. We isolated hepatocytes as previously described [14]. In

brief, the liver cells dispersed by infusing 0.03% collagenase in SC-2 solution were

centrifuged at $50 \times g$ for 1 min. The cell pellet was washed twice by resuspending in

GBSS-B solution (137 mM NaCl, 5.0 mM KCl, 1.0 mM $MgCl_2$, 0.28 mM $MgSO_4$, 0.84

mM NaH_2PO_4, 0.22 mM KH_2PO_4, 5.5 mM glucose, 2.7 mM $NaHCO_3$, and 1.5 mM

CaCl [pH 7.25]) and pelleting at $50 \times g$ for 1 min. We grew the fractionated hepatocytes

using the same method as for HSCs, except that the dishes were coated with type I

collagen.

2.3. Experimental liver fibrosis induced by carbon tetrachloride

As previously reported [5], we injected carbon tetrachloride (CCl_4) (1.0 µl/g body

weight, 25% [v/v] in olive oil) or vehicle alone intraperitoneally into 6-week-old, male

$Sept4^{+/+}$ and $Sept4^{-/-}$ mice, biweekly for 10 weeks.

2.4. Total RNA extraction and DNA microarray analysis

We prepared total RNA from HSCs at the 3rd day in vitro (DIV3) using a

phenol–chloroform extraction method (TRIzol; Invitrogen, Carlsbad, CA) and

monitored the quality of total RNA from the elution profile of 18S and 28S ribosomal

RNA [15] using the Bioanalyzer 2100 (Agilent Technologies, Palo Alto, CA). We

amplified RNA (aRNA) samples using a T7-RNA polymerase system (TargetAmp

1-Round Aminoallyl aRNA amplification kit; Epicentre, Madison, WI) and labeled the

aRNA samples using Cy5 Mono-Reactive Dye Pack (GE Healthcare, England). We

hybridized DNA microarray chips (3D-Gene Mouse Oligo chip 24k; Toray, Tokyo,

Japan) with Cy-5-labeled aRNA samples at 37°C for 16 h and then washed the chips

thoroughly. We scanned the hybridized chips and acquired chip image data using

ProScanArray (Perkin Elmer, Waltham, MA). The scanned image data were processed

using Genepix Pro 4.0 software (Molecular Devices, Sunnyvale, CA) to extract gene

expression data, which were normalized using MATLAB software (Mathworks, Natick,

MA) and a quantile normalization method [16]. For the above procedures, we followed

the manufacturers' protocols with some modifications. We have registered the

microarray data with NCBI's Gene Expression Omnibus (GEO) database under the

accession number GSE24588.

2.5. Quantitative reverse transcription polymerase chain reaction analysis

Total RNA was extracted from liver samples or fractioned liver cells using TRIzol

and reverse transcribed into cDNA using Omniscript RT Kit (QIAGEN, Germantown,

MD) with random primers (Invitrogen). We conducted quantitative reverse transcription

polymerase chain reaction (qRT-PCR) with gene-specific PCR primers (Table 1) and

SYBR Green I Master reaction mix on a LightCycler 480 II (Roche Diagnostics, Basel,

Switzerland). We quantified the relative abundance of each gene product against *18S* as

internal controls with the LightCycler 480 software (ver. 1.5).

2.6. Immunoblot analysis

We homogenized and sonicated cells or tissues in lysis buffer (50 mM Tris-HCl,

2% sodium dodecyl sulfate, and 10% glycerol), and centrifuged the homogenates at

$15,000 \times g$ for 10 min. After measuring the protein concentration and adding

bromophenol blue (final concentration, 0.1%) and 2-mercaptoethanol (5%), each sample

was separated by sodium dodecyl sulfate-polyacrylamide gel electrophoresis

(SDS-PAGE), transferred onto a polyvinylidene fluoride (PVDF) membrane (Hybond-P,

GE Healthcare), and probed with primary antibodies (anti-Dkk2, anti-desmin,

anti-FLAG M2; SIGMA-Aldrich, St. Louis, MO; anti-albumin, BETHYL; Montgomery,

TX, anti-PECAM-1, anti-β-actin; Santa Cruz Biotechnology, Santa Cruz, CA). After

incubation with horseradish peroxidase-conjugated secondary antibodies (Santa Cruz

Biotechnology) and chemiluminescence reaction with the ECL kit (GE Healthcare), we

quantified the luminescence using an image analyzer, LAS-4000 (FujiFilm, Tokyo,

Japan).

2.7. Construction of an expression plasmid for FLAG-Dkk2

We amplified the coding region of a mouse *Dkk2* cDNA clone from the FANTOM

collection (RIKEN) by PCR with a set of oligonucleotide primers, i.e.,

5′-GAGAGAAGCTTTCACAGCTAGGCAGCTCG-3′ and

5′-CGGGATCCTCAGATCTTCTGGCATAC-3′. The *Hin*dIII-*Bam*HI-digested fragment

was inserted in-frame into the cognate sites of an expression plasmid, pFLAG-CMV1,

(SIGMA-Aldrich) and the DNA sequence was confirmed. The FLAG-tag of this vector

is preceded by a signal sequence for secretion and a signal peptidase cleavage site. We

used the empty pFLAG-CMV1 plasmid as a control.

2.8. LX-2 cell culture, transfection, and FLAG-Dkk2 conditioned medium

We cultured 5.0×10^5 LX-2 cells [17] (a generous gift from Dr. Friedman and Dr.

Ikeda) per 60-mm dish in DMEM supplemented with 10% FBS. After about 24 h, we

transfected the cells with the FLAG-Dkk2 or empty plasmid using FuGENE6 (Roche

Diagnostics). We collected the culture supernatant (conditioned medium) containing

recombinant FLAG-Dkk2 or FLAG-tag ~72 h after transfection.

2.9. Immunoprecipitation

We incubated the culture supernatant of the transfected LX-2 cells with

anti-FLAG M2 antibody (SIGMA-Aldrich), followed by adsorption with Protein G

Sepharose beads (GE Healthcare) for 2 h. After washing the beads 3 times with TNE

buffer (10 mM Tris-HCl at pH 7.8, 1% NP40, 0.15 M NaCl, and 1 mM EDTA), we

subjected the immunoprecipitates to immunoblot analysis as described above (section

2.6.).

2.10. Luciferase assay

As described above (section **2.8.**), we seeded 5.0×10^4 LX-2 cells into each well

of 12-well plates and co-transfected the cells with the reporter plasmid TOP-Flash

(Upstate; Millipore), which is designed to monitor the Lef/Tcf-mediated transactivation

of firefly luciferase (emission, 556 nm) [18], and the pGL4.74 [*hRluc*/TK] vector

(Promega, Madison, WI) encoding *Renilla* luciferase (emission, 480 nm) to evaluate the

transfection efficiency. After 24 h, we added the conditioned medium (final

concentration, >90%) containing FLAG-tagged mouse Dkk2 or FLAG-tag alone, or

recombinant Dkk2 (nominal concentration, 5 µg/ml [184 nM]; R&D SYSTEMS, Inc.,

Minneapolis, MN). At 48 h after addition of the conditioned medium, we measured the

activities of the 2 luciferases expressed in LX-2 cells using a Dual-Luciferase Reporter

Assay System (Promega) and a Fluoroskan Ascent FL (Thermo Scientific, Waltham,

MA), according to the manufacturers' instructions. We normalized the data by dividing

the luminescence of the firefly luciferase by that of the *Renilla* luciferase. The

experiments were performed in triplicate.

2.11. Immunohistochemistry of human liver tissues

We procured human tissue specimens of livers afflicted with chronic hepatitis,

liver fibrosis, or liver cirrhosis from the Department of Surgery, Kyoto University

Hospital. All samples were obtained with the patients' informed consent. We

immunostained paraffin sections with anti-Dkk2 antibody (Abcam, Cambridge, UK) as

described previously [5, 14] and observed them under a digital microscope (BZ-9000;

KEYENCE, Japan).

2.12. Statistical analysis

Quantitative data are expressed as mean ± SEM. For statistical analysis, we used

Mann–Whitney's *U* test and a general linear model with repeated measures.

3. Results

3.1. Comparative transcriptome analysis revealed significant reduction of *Dkk2* expression in *Sept4*$^{-/-}$ HSCs

To investigate the molecular mechanism underlying the accelerated transdifferentiation of *Sept4*$^{-/-}$ HSCs [5], we compared the expression profiles of *Sept4*$^{+/+}$ and *Sept4*$^{-/-}$ HSCs cultured in vitro for 3 days (DIV3). DNA microarray analysis showed that the 2 expression profiles did not show a marked difference, but several genes were expressed aberrantly in *Sept4*$^{-/-}$ HSCs (Fig. 1, Tables 2A and 2B, Suppl. Tables 2A, 2B). Among the genes whose differential expression was confirmed by qRT-PCR (see below), we focused on *Dkk2* whose expression was significantly reduced in *Sept4*$^{-/-}$ HSCs. *Dkk2* is a member of the *Dkk* gene family (*Dkk1-5*), each encoding a secretory Wnt antagonist that interacts with the Wnt-Fzd complex by binding to and internalizing LRP5/6, a co-receptor of Fzd [10-12]. Previous studies showed that some Dkks are implicated in the negative regulation of Wnt-mediated cell proliferation, inflammation, and/or pro-fibrotic reactions in diverse tissues, including the liver [8, 9, 19].

3.2. Loss of *Sept4* suppresses upregulation of *Dkk1*, *2*, *3* in an in vivo model of

hepatitis/fibrosis

We tested whether the reduced *Dkk2* expression in cultured *Sept4*$^{-/-}$ HSCs is an in vitro artifact or a pathologically relevant recapitulation of a molecular event during hepatitis and fibrosis. We applied the CCl$_4$ model of hepatitis/fibrosis to *Sept4*$^{-/-}$ and *Sept4*$^{+/+}$ mice as reported previously [5], and quantified the expression levels of 3 major *Dkk* genes expressed in the liver by qRT-PCR. While the basal expression levels of *Dkk1–3* were comparable between the 2 genotypes (controls in Fig. 2A-C), their upregulation after CCl$_4$-induced liver damage was diminished in the absence of *Sept4*. Concordantly, the reduction of Dkk2 upregulation in *Sept4*$^{-/-}$ liver was observed at the protein level (Fig. 2D). Since Dkks are responsible for the suppressive modulation of Wnt-mediated inflammatory/fibrotic processes [8], their reduction in *Sept4*$^{-/-}$ liver may contribute to the enhanced pathological reaction shown previously [5].

3.3. HSCs are the major source of Dkk1–3 in the liver

To identify the origin of upregulated *Dkk1–3* mRNA in vivo, we fractionated wildtype mouse liver cells into 4 populations (i.e., hepatocytes, HSCs, endothelial cells [ECs,] and KCs) and measured the expression of *Dkk1–3* at DIV3 by qRT-PCR. *Dkk1–3* were almost exclusively expressed in HSCs, indicating that HSCs are the major source

of Dkk1–3 secreted in the liver, but hepatocytes and the other cell types are not (Fig.3

A–C, and data not shown). Concordantly, immunoblot analysis showed that Dkk2

protein was almost exclusively expressed in HSCs, but not in hepatocytes, ECs, and

KCs (Fig. 3D). Since Sept4 is also expressed exclusively in HSCs in the liver [5], the

diminished upregulation of *Dkk1–3* is likely to be a cell-autonomous, if not a direct,

consequence of the loss of Sept4.

3.4. Loss of *Sept4* suppresses robust upregulation of *Dkk2/3* through

myofibroblastic transformation of HSCs in vitro

So far, we have demonstrated that the upregulation of *Dkk1–3* is an HSC-specific,

pathologically relevant event that may antagonize the inflammatory/fibrotic processes

mediated by the Wnt pathway. To test whether the 3 major *Dkk* genes are differentially

regulated during myofibroblastic transformation, we examined the time course of their

expression in HSCs cultured in vitro for 1–5 days by qRT-PCR (Fig. 4). Consistent with

the in vivo results (Fig. 2), *Dkk2* and *Dkk3* were remarkably upregulated in this in vitro

model, and more importantly, the upregulation was significantly diminished in *Sept4$^{-/-}$*

HSCs.

3.5. Dkk2 interferes with the canonical Wnt pathway in human HSC-derived cells

Because Dkks are secretory proteins that interact with the Wnt–Fzd complex [7, 20], it is important to test whether or not Dkks produced by HSCs can act on HSCs in an autocrine/paracrine manner. Since primary cultured HSCs are unsuitable for the following assay which requires a high transfection efficiency, we employed a human HSC-derived cell line, LX-2 [17]. We transfected LX-2 cells either with a FLAG-tagged mouse Dkk2 expression plasmid or with an empty (FLAG-tag alone) plasmid, which served as a control. The culture supernatant from each condition was collected 3 days after transfection, immunoprecipitated with an anti-FLAG M2 antibody, and immunoblotted for Dkk2. The immunoblot showed a 28-kDa polypeptide for FLAG-Dkk2 secreted into the medium (Fig. 5A).

To test whether Dkk2 could interfere with the canonical Wnt signaling pathway in HSCs, we transfected LX-2 cells with a TOP-Flash reporter plasmid, which is designed to monitor the activity of the canonical Wnt pathway through Lef/Tcf-mediated luciferase gene expression [18]. The reporter-transfected LX-2 cells were supplemented with the aforementioned conditioned medium with or without FLAG-Dkk2. Compared with the control medium, the FLAG-Dkk2-containing medium significantly suppressed the luciferase activity of LX-2 cells measured 2 days later (Fig. 5B). Taken together,

these data indicate that Dkks secreted from HSCs act on HSCs in an autocrine/paracrine manner and interfere with the canonical Wnt pathway, which is known to drive myofibroblastic transformation [9]. However, these data do not exclude the possibility that Dkks suppress the non-canonical Wnt signaling pathways in HSCs or act on other cell types in the liver.

3.6. Dkk2 interferes with pro-fibrotic transformation of *Sept4*$^{-/-}$ HSCs

On the basis of the above results, we examined whether supplementing exogenous Dkk2 could mitigate the accelerated fibrotic transformation of *Sept4*$^{-/-}$ HSCs. We isolated HSCs from *Sept4*$^{-/-}$ mice and cultured them with FLAG-Dkk2-containing or control medium. After 3 days, we measured the expression of representative markers by qRT-PCR: the pro-fibrotic genes *α-Sma*, *Colα 1*, and *Col3α1* (the major collagen genes in the liver) and an anti-fibrotic gene, *Smad7*, which encodes an inhibitor of the transforming growth factor (TGF)-β /Smad3 pathway. The FLAG-Dkk2-containing medium downregulated the expression of *α-Sma*, *Col1α1*, and *Col3α1*, and upregulated the expression of *Smad7* in *Sept4*$^{-/-}$ HSCs (Fig. 6). Concordantly, one-shot supplementation of recombinant Dkk2 (nominal concentration, 5 µg/ml [184 nM]) gave similar but less significant results, partly due to its low actual potency and/or rapid

clearance (Suppl. Fig 1). These data indicate that continuous supplementation with

Dkk2 can partially suppress the myofibroblastic transformation of *Sept4*$^{-/-}$ HSCs by

interfering with the canonical Wnt signaling pathway that transactivates pro-fibrotic

genes and suppresses the expression of anti-fibrotic genes.

3.7. Status of Dkk2 in human HSCs under pathological conditions

We assessed the clinical relevance of our findings by determining the status of

Dkk2 in pathological human liver specimens using immunohistochemistry. There was a

gradual increment of Dkk2-immunoreactivity from normal liver tissue, hepatitis, mild

fibrosis through to cirrhosis (Fig. 7A–D). Dkk2-positive cells were detected almost

exclusively in the perisinusoidal spaces where HSCs reside, and appeared to increase in

number as fibrosis progressed. These data conform to the hypothesis that the

upregulation of Dkk2 in HSCs is a common counteractive mechanism against fibrotic

processes in liver diseases.

4. Discussion

This study derived from an open question raised by our previous findings [5], which included the determination of the mechanism that renders *Sept4*$^{-/-}$ mice prone to liver fibrosis. Genome-wide expression profiling and qRT-PCR analysis revealed that a number of genes in HSCs are expressed differently in the absence of *Sept4*. We hypothesized that these include genes responsible for the fibrosis-prone phenotype. In this report, we focused on the reduced expression of the anti-fibrotic genes *Dkk1–3* in *Sept4*$^{-/-}$ HSCs. Supplementation with recombinant Dkk2 partially corrected the aberrant gene expression profile in *Sept4*$^{-/-}$ HSCs by downregulating the pro-fibrotic genes *α-Sma, Col1α1* and *Col3α1* and upregulating the anti-fibrotic gene *Smad7* (Fig. 6, Suppl. Fig. 1). These data indicate that the scarcity of Dkks is a major, if not the sole, determinant of the fibrosis-prone phenotype of *Sept4*$^{-/-}$ mice, partly resolving the initial question. Other differentially expressed genes include downstream targets of the canonical Wnt pathway (Suppl. Table 2A and B), although their contribution has not been assessed in this study.

The molecular network of Wnt signaling consists of 3 major pathways, i.e., the canonical Wnt/β-catenin pathway, the Wnt/Ca^{2+} pathway, and the planar cell polarity–convergent extension pathway. The canonical Wnt pathway plays a critical role

in developmental morphogenesis and homeostatic tissue remodeling by controlling cell

proliferation and differentiation [7, 11]. Hence, dysregulation of this pathway is known

to cause cancer [21], aberrant tissue remodeling [22, 23], and fibrosis [6]. This pathway

is activated when Wnt binds to its cognate receptor Fzd, which interacts with the

glycogen synthase kinase-3 β-mediated phosphorylation and the subsequent degradation

of β-catenin. When β-catenin translocates to the nucleus, it activates the transcription

factor Lef/Tcf and alters the gene expression pattern. Dkks interact with the canonical

Wnt pathway by binding to and facilitating the internalization of LRP5/6, a co-receptor

of Fzd [10]. Among the 3 major Dkk family members expressed in HSCs, Dkk1

consistently antagonizes the canonical Wnt pathway, while Dkk2 can be either an

antagonist or an agonist, depending on the presence or absence of another Wnt

co-receptor, Kremen1/2 [24]. The expression of *Kremen1/2* in HSCs (Suppl. Fig. 2) is

consistent with the antagonistic function of Dkk2 in the canonical Wnt pathway (Fig. 5).

Thus, Dkk1/2 may antagonize the canonical Wnt pathway in HSCs, though the function

of Dkk3 is currently unclear.

Open questions also include the molecular mechanism that links loss of Sept4 and

reduced transactivation of the *Dkk* genes (Fig. 8). Since Sept4 is a subunit of the septin

heteropolymers associated mainly with other cytoskeletal and submembranous

components (see Fig. 1 [5]), its direct interaction with the transcription machinery is unlikely. In some human cell lines, however, depletion of the Sept7 subunit can release suppressor of cytokine signaling 7 (SOCS7) from septin heteropolymers in the cytoplasm, which promotes the translocation of the non-catalytic region of tyrosine kinase adaptor protein (NCK) to the nucleus and activates the DNA damage checkpoint machinery [25]. Thus, genetic loss of Sept4 could also indirectly alter nuclear events. Another scenario similar to the scarcity of the dopamine transporter in $Sept4^{-/-}$ dopamine neurons [3] is that some proteins responsible for anti-fibrotic signaling could be destabilized by the loss of septin-based scaffolds in $Sept4^{-/-}$ HSCs. Narrowing down the molecular mechanism from these and other possibilities should give us a clearer picture of myofibroblastic transformation of HSCs in liver fibrosis.

Supplementary materials related to this article can be found online 412 at doi:10.1016/j.bbadis.2011.06.015.

5. Acknowledgements

6. Grants

References

[1]   S.L. Friedman, Hepatic fibrosis - overview, Toxicology 254 (2008) 120-129.

[2]   S.L. Friedman, Mechanisms of hepatic fibrogenesis, Gastroenterology 134

        (2008) 1655-1669.

[3]   M. Ihara, N. Yamasaki, A. Hagiwara, A. Tanigaki, A. Kitano, R. Hikawa, H.

        Tomimoto, M. Noda, M. Takanashi, H. Mori, N. Hattori, T. Miyakawa, M.

        Kinoshita, Sept4, a component of presynaptic scaffold and Lewy bodies, is

        required for the suppression of alpha-synuclein neurotoxicity, Neuron 53 (2007)

        519-533.

[4]   M. Ihara, A. Kinoshita, S. Yamada, H. Tanaka, A. Tanigaki, A. Kitano, M. Goto,

        K. Okubo, H. Nishiyama, O. Ogawa, C. Takahashi, S. Itohara, Y. Nishimune, M.

        Noda, M. Kinoshita, Cortical organization by the septin cytoskeleton is essential

        for structural and mechanical integrity of mammalian spermatozoa, Dev Cell 8

        (2005) 343-352.

[5]   K. Iwaisako, E. Hatano, K. Taura, A. Nakajima, M. Tada, S. Seo, N. Tamaki, F.

        Sato, I. Ikai, S. Uemoto, M. Kinoshita, Loss of Sept4 exacerbates liver fibrosis

        through the dysregulation of hepatic stellate cells, J Hepatol 49 (2008) 768-778.

[6]   I. Hwang, E.Y. Seo, H. Ha, Wnt/beta-catenin signaling: a novel target for

therapeutic intervention of fibrotic kidney disease, Arch Pharm Res 32 (2009) 1653-1662.

[7]   C. Prunier, B.A. Hocevar, P.H. Howe, Wnt signaling: physiology and pathology, Growth Factors 22 (2004) 141-150.

[8]   J.H. Cheng, H. She, Y.P. Han, J. Wang, S. Xiong, K. Asahina, H. Tsukamoto, Wnt antagonism inhibits hepatic stellate cell activation and liver fibrosis, Am J Physiol Gastrointest Liver Physiol 294 (2008) G39-49.

[9]   S.J. Myung, J.H. Yoon, G.Y. Gwak, W. Kim, J.H. Lee, K.M. Kim, C.S. Shin, J.J. Jang, S.H. Lee, S.M. Lee, H.S. Lee, Wnt signaling enhances the activation and survival of human hepatic stellate cells, FEBS Lett 581 (2007) 2954-2958.

[10]   Y. Kawano, R. Kypta, Secreted antagonists of the Wnt signalling pathway, J Cell Sci 116 (2003) 2627-2634.

[11]   W. Wu, A. Glinka, H. Delius, C. Niehrs, Mutual antagonism between dickkopf1 and dickkopf2 regulates Wnt/beta-catenin signalling, Curr Biol 10 (2000) 1611-1614.

[12]   A. Niida, T. Hiroko, M. Kasai, Y. Furukawa, Y. Nakamura, Y. Suzuki, S. Sugano, T. Akiyama, DKK1, a negative regulator of Wnt signaling, is a target of the beta-catenin/TCF pathway, Oncogene 23 (2004) 8520-8526.

[13] R. Weiskirchen, A.M. Gressner, Isolation and culture of hepatic stellate cells, Methods Mol Med 117 (2005) 99-113.

[14] N. Tamaki, E. Hatano, K. Taura, M. Tada, Y. Kodama, T. Nitta, K. Iwaisako, S. Seo, A. Nakajima, I. Ikai, S. Uemoto, CHOP deficiency attenuates cholestasis-induced liver fibrosis by reduction of hepatocyte injury, Am J Physiol Gastrointest Liver Physiol 294 (2008) G498-505.

[15] B.A. Centeno, S.A. Enkemann, D. Coppola, S. Huntsman, G. Bloom, T.J. Yeatman, Classification of human tumors using gene expression profiles obtained after microarray analysis of fine-needle aspiration biopsy samples, Cancer 105 (2005) 101-109.

[16] B.M. Bolstad, R.A. Irizarry, M. Astrand, T.P. Speed, A comparison of normalization methods for high density oligonucleotide array data based on variance and bias, Bioinformatics 19 (2003) 185-193.

[17] L. Xu, A.Y. Hui, E. Albanis, M.J. Arthur, S.M. O'Byrne, W.S. Blaner, P. Mukherjee, S.L. Friedman, F.J. Eng, Human hepatic stellate cell lines, LX-1 and LX-2: new tools for analysis of hepatic fibrosis, Gut 54 (2005) 142-151.

[18] D. Sakai, Y. Tanaka, Y. Endo, N. Osumi, H. Okamoto, Y. Wakamatsu, Regulation of Slug transcription in embryonic ectoderm by beta-catenin-Lef/Tcf and

BMP-Smad signaling, Dev Growth Differ 47 (2005) 471-482.

[19]   M.D. Thompson, S.P. Monga, WNT/beta-catenin signaling in liver health and

disease, Hepatology 45 (2007) 1298-1305.

[20]   A.M. Zorn, Wnt signalling: antagonistic Dickkopfs, Curr Biol 11 (2001)

R592-595.

[21]   B.T. MacDonald, K. Tamai, X. He, Wnt/beta-catenin signaling: components,

mechanisms, and diseases, Dev Cell 17 (2009) 9-26.

[22]   R. Baron, G. Rawadi, Targeting the Wnt/beta-catenin pathway to regulate bone

formation in the adult skeleton, Endocrinology 148 (2007) 2635-2643.

[23]   X. Li, P. Liu, W. Liu, P. Maye, J. Zhang, Y. Zhang, M. Hurley, C. Guo, A.

Boskey, L. Sun, S.E. Harris, D.W. Rowe, H.Z. Ke, D. Wu, Dkk2 has a role in

terminal osteoblast differentiation and mineralized matrix formation, Nat Genet

37 (2005) 945-952.

[24]   B. Mao, C. Niehrs, Kremen2 modulates Dickkopf2 activity during Wnt/LRP6

signaling, Gene 302 (2003) 179-183.

[25]   B.E. Kremer, L.A. Adang, I.G. Macara, Septins regulate actin organization and

cell-cycle arrest through nuclear accumulation of NCK mediated by SOCS7, Cell 130

(2007) 837-850.

Figure legends

Figure 1: Comparative genome-wide expression profiling between *Sept4*$^{+/+}$ and

***Sept4*$^{-/-}$ hepatic stellate cells**

Two-dimensional scatter plot showing comparative transcriptome data obtained

using a DNA microarray system (23,474 probes; Mouse Oligo chip, Toray, Tokyo,

Japan). Each dot represents the amount of mRNA obtained from *Sept4*$^{+/+}$ hepatic

stellate cells (HSCs) (horizontal axis) and *Sept4*$^{-/-}$ HSCs (vertical axis) on a log$_2$-based

scale. The quality of mRNA and the reproducibility of these experiments are

corroborated by compact clustering of the dots along the diagonal. The results were

confirmed by triplicate measurements. The genes that prominently deviated from the

diagonal are listed in Tables 2A and 2B. This study focused on *Dkk2* whose reduced

expression in *Sept4*$^{-/-}$ HSCs was confirmed by quantitative reverse transcription

polymerase chain reaction (qRT-PCR) (see below).

Figure 2: Genetic loss of *Sept4* affects induced expression patterns of *Dkk* genes in

an in vivo model of hepatitis and liver fibrosis

(A–C) Quantitative reverse transcription polymerase chain reaction (RT-PCR)

showed that the basal expression level of the 3 major *Dkk* genes in the liver, *Dkk1-3*,

were comparable between *Sept4*$^{+/+}$ and *Sept4*$^{-/-}$ hepatic stellate cells (HSCs), whereas

their upregulation upon CCl_4-induced liver damage was diminished in the absence of

Sept4. The data are shown as mean ± SEM (n = 6; *Dkk1*: p = 0.35, *Dkk2*: p = 0.037*,

Dkk3: p = 0.005** by Mann‑Whitney's *U* test).

(D) A representative immunblot image showing that a *Sept4*$^{-/-}$ mouse liver with

CCl_4-induced hepatitis and fibrosis contains significantly lower amounts of Dkk2

protein as compared with a wildtype (*Sept4*$^{+/+}$) control. The data are shown as mean ±

SEM (n = 4, p = 0.021* by Mann‑Whitney's *U* test).

Figure 3: Hepatic stellate cells are the major source of Dkk1−3 in the liver

(A–C) Hepatocytes and hepatic stellate cells (HSCs) were fractionated from

wildtype mouse liver specimens, and *Dkk1-3* expressions were measured by quantitative

reverse transcription polymerase chain reaction (qRT-PCR). The data from duplicate

experiments are shown as mean ± SEM (n = 5, *Dkk1*: p = 0.006**, *Dkk2*: p = 0.006**,

Dkk3: p = 0.005**).

(D) Immunoblot analysis showed that Dkk2 was abundant in the HSC fraction but

not in the hepatocyte and endothelial cell plus Kupffer cell fractions.

Figure 4: *Dkk2/3* are upregulated upon myofibroblastic transformation of hepatic

stellate cells and the induction is diminished by loss of *Sept4*

The time course of *Dkk1−3* expression in hepatic stellate cells (HSCs) cultured for

1−5 days was estimated by quantitative reverse transcription polymerase chain reaction

(qRT-PCR). The remarkable upregulation of *Dkk2* and *Dkk3* found in *Sept4*$^{+/+}$ HSCs

was significantly diminished in *Sept4*$^{-/-}$ HSCs. Data from duplicate experiments are

shown as mean ± SEM (*Sept4*$^{+/+}$: n = 6, *Sept4*$^{-/-}$: n = 4; *Dkk1*: p = 0.49, *Dkk2*: p <

0.020*, *Dkk3*: p = 0.057 by a general linear model with repeated measures).

Figure 5: Dkk2 can interfere with the canonical Wnt pathway of human hepatic

stellate cell-derived LX-2 cells

(A) FLAG-tagged Dkk2 expressed in LX-2 cells and released to the culture

supernatant was immunoprecipitated with anti-FLAG M2 antibody and immunoblotted

for Dkk2.

(B) LX-2 cells transfected with the TOP-Flash reporter plasmid were incubated

with the conditioned medium containing FLAG-Dkk2 or FLAG alone and analyzed in a

dual luciferase assay. FLAG-Dkk2 significantly suppressed the transactivation of the

reporter gene encoding firefly luciferase, indicative of its interaction with the canonical

Wnt pathway. Data from duplicate experiments are shown as mean ± SEM (n = 5, p =

0.033*).

Figure 6: Dkk2 interferes with myofibroblastic transformation of *Sept4*$^{-/-}$ hepatic stellate cells

    Sept4$^{-/-}$ hepatic stellate cells (HSCs) were supplemented with FLAG-Dkk2, and the expressions of representative pro-fibrotic and anti-fibrotic markers were measured by quantitative reverse transcription polymerase chain reaction (qRT-PCR). The pro-fibrotic markers *α-Sma* (p = 0.001), *Col1α1* (p = 0.005), and *Col3α1* (p = 0.001) were significantly downregulated in the presence of FLAG-Dkk2, while *Smad7* (p = 0.011) was significantly upregulated. Data from duplicate experiments are shown as mean ± SEM (n = 6, *: p < 0.05, **: p < 0.01). In conjunction with the above results (Fig. 5), these data indicate that supplementation with Dkk2 can mitigate myofibroblastic transformation of *Sept4*$^{-/-}$ HSCs by interaction with the canonical Wnt signaling pathway that transactivates pro-fibrotic genes and suppresses the expression of anti-fibrotic genes.
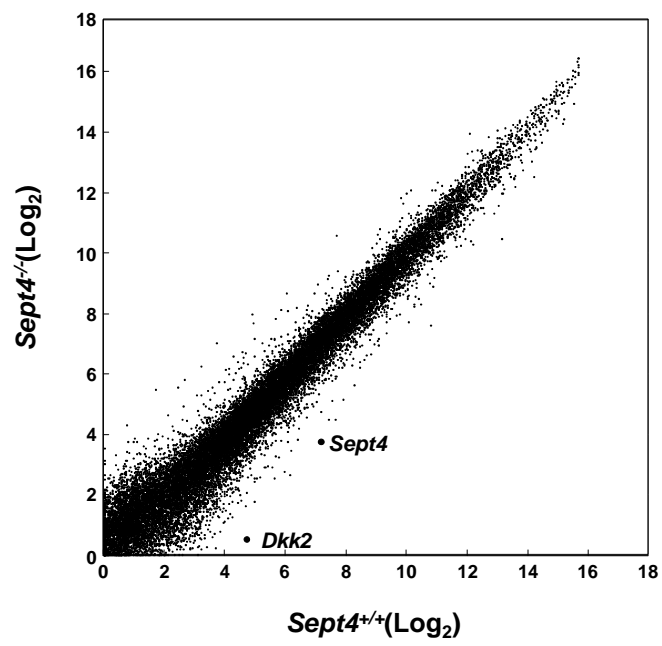
Figure 7: Dkk2 is upregulated in human hepatic stellate cells under pathological conditions
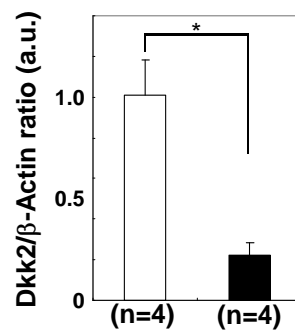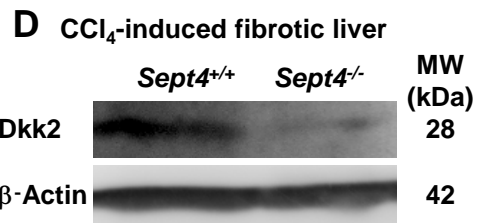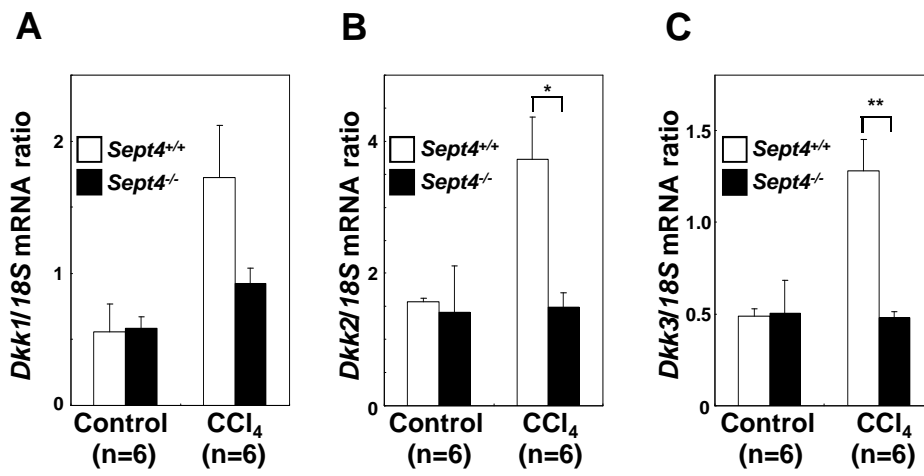
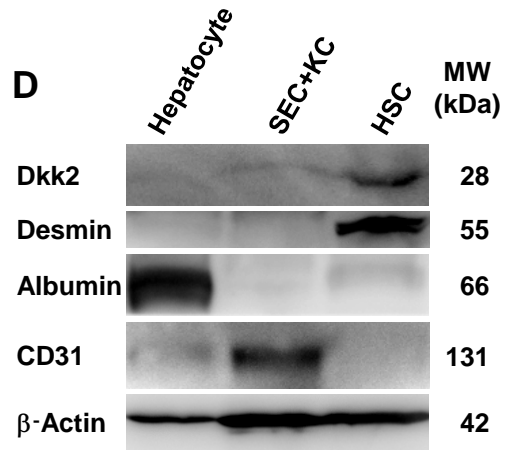   Immunohistochemistry of Dkk2 in human liver specimens. Dkk2-positive cells
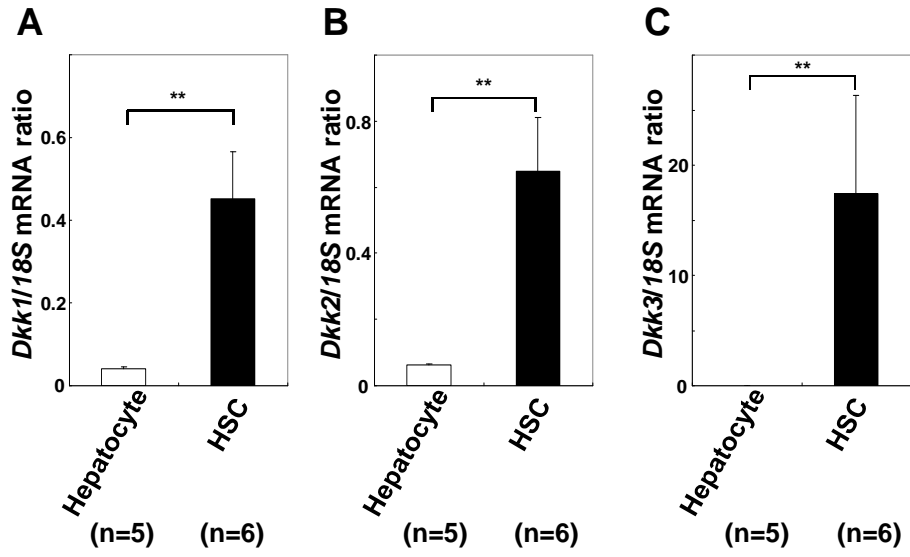
(brown stain) were detected almost exclusively in the perisinusoidal spaces where

hepatic stellate cells (HSCs) reside. The level of Dkk2-immunoreactivity appeared to be

positively correlated with the progression of fibrosis from normal liver tissue (A), HCV

hepatitis (B), mild fibrosis (C) through to cirrhosis (D). These data conform to the idea

that Dkk2 upregulation in HSCs is a common counteractive mechanism against fibrotic

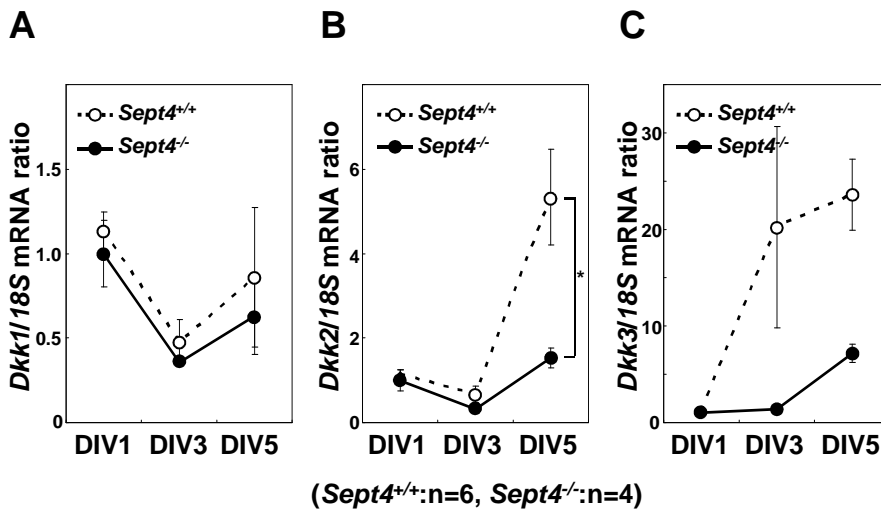processes conserved across species.

Figure 8: *Sept4* is required to boost the induction of Dkks that counteract

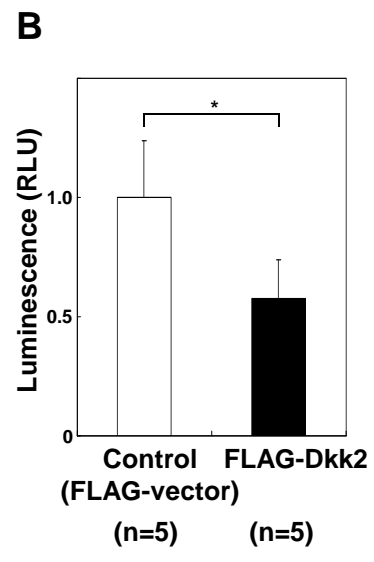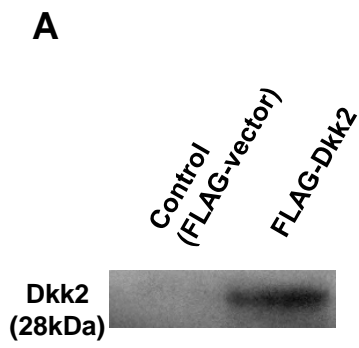**myofibroblastic transformation of hepatic stellate cells**

A schematic diagram showing the involvement of Sept4 in the molecular network

underlying the liver fibrosis-prone phenotype of $Sept4^{-/-}$ mice. The canonical Wnt

pathway promotes myofibroblastic transformation of HSCs by transactivating

pro-fibrotic genes and suppressing anti-fibrotic genes, which is counteracted by Dkks.

This study revealed the involvement of *Sept4* as an epistatic factor that boosts the

upregulation of Dkks by unknown mechanism. The missing link between *Sept4* and *Dkk*

induction has become a focus of future studies on the molecular pathophysiology of

liver fibrosis.

A

Dkk1/18S mRNA ratio

□ Sept4+/+
■ Sept4-/-

Control (n=6)   CCl₄ (n=6)

B

Dkk2/18S mRNA ratio

□ Sept4+/+
■ Sept4-/-

*

Control (n=6)   CCl₄ (n=6)

C

Dkk3/18S mRNA ratio

□ Sept4+/+
■ Sept4-/-

**

Control (n=6)   CCl₄ (n=6)

D CCl₄-induced fibrotic liver

Sept4+/+   Sept4-/-   MW (kDa)

Dkk2   28

β-Actin   42

Dkk2/β-Actin ratio (a.u.)

*

(n=4)   (n=4)

A

$Dkk1/18S$ mRNA ratio

Hepatocyte (n=5)   HSC (n=6)

**

B

$Dkk2/18S$ mRNA ratio

Hepatocyte (n=5)   HSC (n=6)

**

C

$Dkk3/18S$ mRNA ratio

Hepatocyte (n=5)   HSC (n=6)

**

D

	Hepatocyte	SEC+KC	HSC	MW (kDa)
Dkk2				28
Desmin				55
Albumin				66
CD31				131
β-Actin				42

A

Dkk1/18S mRNA ratio

○ *Sept4⁺/⁺*
● *Sept4⁻/⁻*

DIV1 DIV3 DIV5

B

Dkk2/18S mRNA ratio

○ *Sept4⁺/⁺*
● *Sept4⁻/⁻*

DIV1 DIV3 DIV5

C

Dkk3/18S mRNA ratio

○ *Sept4⁺/⁺*
● *Sept4⁻/⁻*

DIV1 DIV3 DIV5

(*Sept4⁺/⁺*:n=6, *Sept4⁻/⁻*:n=4)

A

Dkk2
(28kDa)

Control (FLAG-vector)

FLAG-Dkk2

B

Luminescence (RLU)

1.0

0.5

0

*

Control
(FLAG-vector)
(n=5)

FLAG-Dkk2
(n=5)

A

α-Sma/18S mRNA ratio

1.0

0.5

0

**

Control
(FLAG-vector)
(n=6)

FLAG-Dkk2

(n=6)

B

Col1α1/18S mRNA ratio

1.0

0.5

0

**

Control
(FLAG-vector)
(n=6)

FLAG-Dkk2

(n=6)

C

Col3a1/18S mRNA ratio

1.0

0.5

0

**

Control
(FLAG-vector)
(n=6)

FLAG-Dkk2

(n=6)

D

Smad7/18S mRNA ratio

1.5

1.0

0.5

0

*

Control
(FLAG-vector)
(n=6)

FLAG-Dkk2

(n=6)

A (Normal liver)

B (Hepatitis)

C (Liver fibrosis)

D (Liver cirrhosis)

50μm

Sept4

?

Dkks

Injury

Auto/Paracrine

**Wnt/β-Catenin
Signal in HSCs**

**Myofibroblastic transformation
Pro-fibrotic genes** ↑
Anti-fibrotic genes ↓

Liver fibrosis

Table 1: Primers used quantitative RT-PCR

Primer	Forward	Reverse
α-Sma	GTCCCAGACATCAGGGAGTAA	TCGGATACTTCAGCGTCAGGA
18S	AGTCCCTGCCCTTTGTACACA	CGATCCGAGGGCCTCACTA
Col1α1	GCTCCTCTTAGGGGCCACT	CCACGTCTCACCATTGGGG
Col3α1	CACCCTTCTTCATCCCACTC	TCTCCAAATGGGATCTCTGG
Dkk1	CTCATCAATTCCAACGCGATCA	GCCCTCATAGAGAACTCCCG
Dkk2	CTGATGCGGGTCAAGGATTCA	CTCCCCTCCTAGAGAGGACTT
Dkk3	CTCGGGGGTATTTGCTGTGT	TCCTCCTGAGGGTAGTTGAGA
Smad7	GCATCTTCTGTCCCTGCTTC	CCGGTCTTCCTTTCCTTTTC

Table 2A: Genes downregulated in *Sept4*$^{-/-}$ hepatic stellate cells (10 from the top)

	Gene Symbol	Control (*Sept4*$^{+/+}$) (Log$_2$)	*Sept4*$^{-/-}$ (Log$_2$)	Fold Change	Gene Annotation
1	*Dkk2*	4.79	0.820	0.0640	dickkopf homolog 2
2	*Ivl*	6.22	2.93	0.102	involucrin
3	*Sept4*	7.24	4.02	0.107	septin 4
4	*Ptgs2*	10.9	7.88	0.127	prostaglandin-endoperoxide synthase 2
5	*Acta1*	6.04	3.06	0.127	actin, alpha 1, skeletal muscle
6	*Tll1*	7.72	4.76	0.128	tolloid-like
7	*Kctd11*	3.46	0.556	0.133	potassium channel tetramerisation domain containing 11
8	*Sprrl9*	5.72	2.82	0.135	small proline rich-like 9
9	*Ahrr*	4.77	1.90	0.137	aryl-hydrocarbon receptor repressor
10	*Kcnj5*	3.17	0.317	0.139	potassium inwardly-rectifying channel J5

Table 2B: Genes upregulated in *Sept4*$^{-/-}$ hepatic stellate cells (10 from the top)

	Gene Symbol	Control (*Sept4*$^{+/+}$) (Log$_2$)	*Sept4*$^{-/-}$ (Log$_2$)	Fold Change	Gene Annotation
1	*Nfat5*	0.838	4.60	13.5	nuclear factor of activated T-cells 5
2	*Saa3*	3.81	7.29	11.2	serum amyloid A 3
3	*Gm839*	2.75	6.11	10.2	gene model 839, (NCBI)
4	*Cuedc1*	4.99	8.26	9.70	CUE domain containing 1
5	*Gpr160*	3.29	6.52	9.38	G protein-coupled receptor 160
6	*Gpr103*	0.113	3.30	9.12	G protein-coupled receptor 103
7	*Ntf3*	0.886	4.05	8.98	neurotrophin 3
8	*Akp2*	7.74	10.9	8.74	alkaline phosphatase 2, liver
9	*Slc10a6*	1.08	4.14	8.38	solute carrier family 10, member 6
10	*Hsd3b2*	1.05	4.02	7.85	hydroxysteroid dehydrogenase-2, delta<5>-3-beta

Legend of Tables 2A and 2B

Comparative DNA microarray data of *Sept4*$^{-/-}$ and *Sept4*$^{+/+}$ hepatic stellate cells

(HSCs), showing representative genes whose expression were up- (A) and

downregulated (B) in *Sept4*$^{-/-}$ HSCs. All the data have been deposited to NCBI GEO

under an accession number of GSE24588.

Supplemental Figure 1: Marginal suppression of myofibroblastic transformation of *Sept4*$^{-/-}$ hepatic stellate cells after supplementation with recombinant Dkk2

Sept4$^{-/-}$ hepatic stellate cells (HSCs) at day 1 in vitro (DIV1) were supplemented with recombinant Dkk2 (5 µg/ml [184 nM]) and the expression of representative pro-fibrotic and anti-fibrotic markers was measured 3 days later by quantitative reverse transcription polymerase chain reaction (qRT-PCR). The pro-fibrotic genes *α-Sma* (p = 0.62), *Col1α1* (p = 0.67), and *Col3α1* (p = 0.46) were downregulated in the presence of recombinant Dkk2, while the anti-fibrotic gene *Smad7* (p = 0.47) was upregulated. Although the differences were not statistically significant, the results were concordant with the FLAG-Dkk2 conditioned media experiment (Fig. 6). Data from duplicate experiments are shown as mean ± SEM (n = 6).

Supplemental Figure 2: **Expression of *Kremen1/2* in cultured hepatic stellate cells**

(A, B) The expression of *Kremen1/2* genes in *Sept4*$^{+/+}$ and *Sept4*$^{-/-}$ mouse hepatic stellate cells (HSCs) at days 1 to 5 in vitro (DIV1−5) was assessed by quantitative reverse transcription polymerase chain reaction (qRT-PCR). *Kremen1* was upregulated during myofibroblastic transformation, which was slightly blunted in the absence of *Sept4* (p = 0.12, a general linear model with repeated measures). *Kremen2* was not

induced in this model (p = 0.83). Data from duplicate experiments are shown as mean ±

SEM (n = 4 or 6).

(C, D) *Kremen1/2* expression in *Sept4*$^{-/-}$ HSCs supplemented with FLAG-Dkk2

was quantified by qRT-PCR. FLAG-Dkk2 tended to suppress *Kremen1* expression (p =

0.15, Mann‑Whitney's *U* test), while enhancing *Kremen2* expression (p = 0.38).

Supplemental Figure 3: The culture supernatant of transfected LX-2 cells

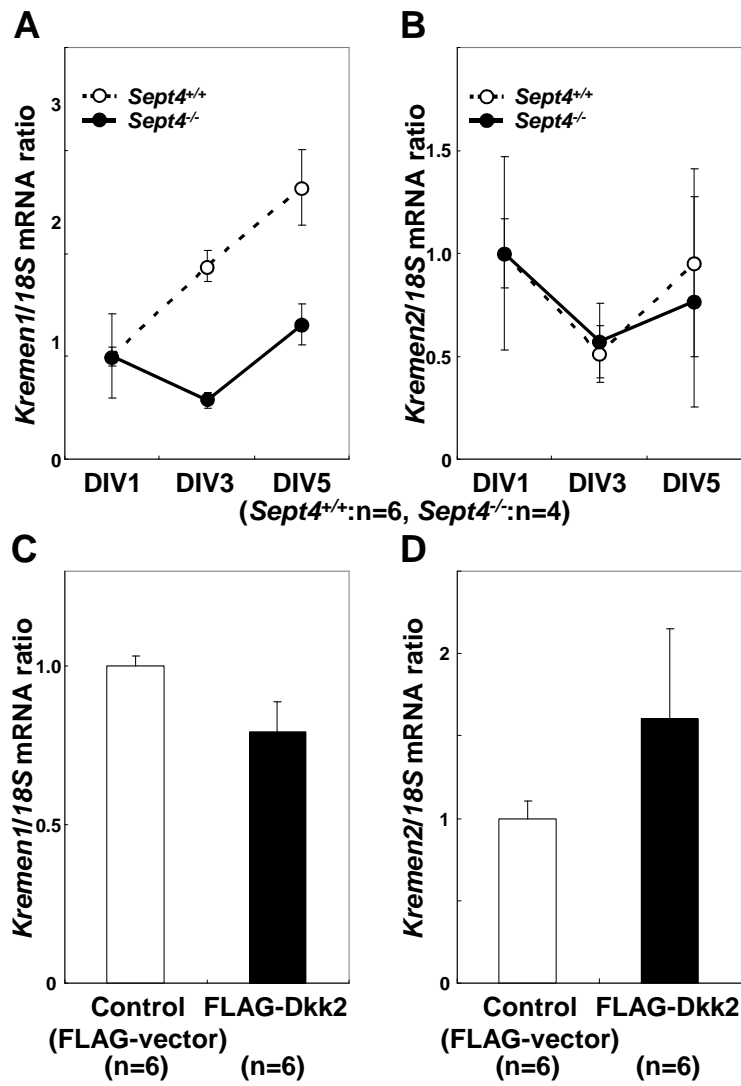**contained FLAG-tagged Dkk2 protein**

FLAG-tagged Dkk2 expressed in LX-2 cells and released to the culture

supernatant was immunoprecipitated with an anti-Dkk2 antibody and immunoblotted

for the FLAG epitope. This is a reciprocal experiment of Fig. 5A.

Supplemental Figure 1
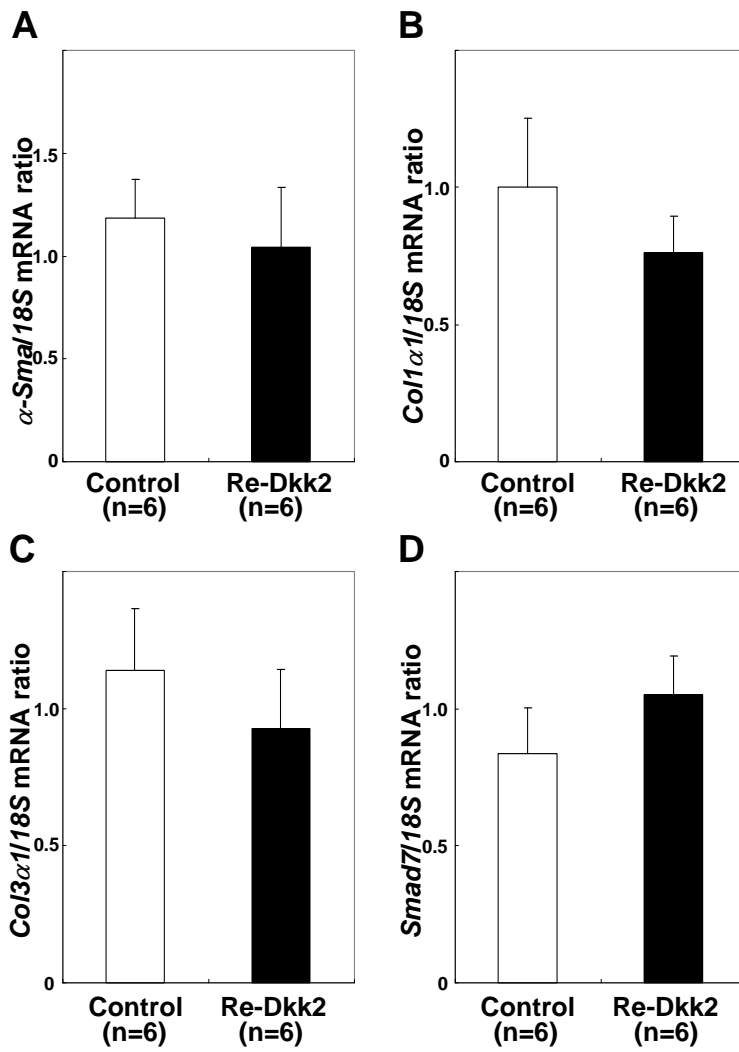
Supplemental Figure 2

Supplemental Figure 3

IP:anti-Dkk2 + IB:anti-FLAG M2